

Minding the gap: testing natural anomaly-mediated SUSY breaking at high luminosity LHC

Howard Baer^{1*}, Vernon Barger^{2†}, Jessica Bolich^{1‡}
 Juhi Dutta^{1§} and Dibyashree Sengupta^{3¶}

¹*Department of Physics and Astronomy, University of Oklahoma, Norman, OK 73019, USA*

²*Department of Physics, University of Wisconsin, Madison, WI 53706, USA*

³*INFN, Laboratori Nazionali di Frascati, Via E. Fermi 54, 00044 Frascati (RM), Italy*

Abstract

While the minimal anomaly-mediated SUSY breaking model (mAMSB) seems ruled out by constraints on Higgs mass, naturalness and wino dark matter, a slightly generalized version dubbed natural AMSB (nAMSB) remains both viable and compelling. Like mAMSB, nAMSB features winos as the lightest gauginos, but unlike mAMSB, nAMSB allows a small μ parameter so that higgsinos are the lightest of electroweakinos (EWinos). nAMSB spectra depend on the input value of gravitino mass $m_{3/2}$, where the lower range of $m_{3/2}$ is excluded by LHC gluino pair searches while a higher $m_{3/2}$ band is excluded by LHC limits on wino pair production followed by boosted hadronic wino decays. A remaining intermediate gap in $m_{3/2}$ values remains allowed by present LHC searches, but appears to be completely explorable by high luminosity upgrades of LHC (HL-LHC). We explore a variety of compelling discovery channels that may allow one to close the intermediate gap in $m_{3/2}$ values: 1. same-sign diboson+ E_T (SSdB) production arising from wino pair production, leading to same-sign dileptons plus missing E_T , 2. trilepton production arising from wino pair production and 3. soft dilepton plus jet events from higgsino pair production, 4. top-squark pair production. From our signal-to-background analysis along a nAMSB model line, we expect HL-LHC to either discover or rule out the nAMSB model with 3000 fb^{-1} of integrated luminosity.

*Email: baer@nhn.ou.edu

†Email: barger@pheno.wisc.edu

‡Email: Jessica.R.Bolich-1@ou.edu

§Email: juhi.dutta@ou.edu

¶Email: Dibyashree.Sengupta@lnf.infn.it

1 Introduction

In gravity-mediated supersymmetry breaking models[1, 2], one posits a visible sector (usually consisting of Minimal Supersymmetric Standard Model or MSSM fields) and a hidden sector which allows for supersymmetry breaking to occur. Under supergravity breaking[3], some hidden sector field X develops a SUSY breaking vev F_X so that the gravitino acquires a mass $m_{3/2} \sim F_X/m_P$ which can be of order the weak scale m_{weak} for $F_X \sim m_{hidden}^2 \sim (10^{11} \text{ GeV})^2$. This can then lead to the generation of visible sector soft SUSY breaking scalar mass-squared m_ϕ^2 , gaugino masses m_λ , trilinear (A) and bilinear (B) terms all of order $m_{3/2}$, which can lead to a 't Hooft technically natural solution[4] of the Standard Model (SM) big hierarchy problem (BHP)[5] and a practical natural solution to the MSSM little hierarchy problem (LHP)[6]. But how can the exponentially suppressed scale $\sqrt{F_X} \ll m_P$ arise? An attractive framework lies in dynamical SUSY breaking (DSB)[7] where non-perturbative breaking, say via hidden sector gaugino condensation[8] where a gauge group (say $SU(N)$) becomes strongly interacting at the intermediate scale leading to $m_{hidden} \sim m_P \exp(-8\pi^2/g_h^2)$, and the hidden sector mass scale arises via dimensional transmutation.

A conundrum with this approach is that gaugino masses and A -terms require hidden sector singlets to develop vevs, and singlets do not seem to have a place within the hidden sector gauge theory[9]. Nonetheless, it was pointed out by Randall-Sundrum[10] and Giudice *et al.*[11] that these terms could arise with loop suppressed values which trace back to the superconformal anomaly, thus dubbed as anomaly-mediated SUSY breaking (AMSB) terms. In this case, gaugino masses arise as

$$M_i = \frac{\beta_{g_i}}{g_i} m_{3/2} \quad (1)$$

where i labels the corresponding gauge group and β_{g_i} is its β function. A_f terms develop as $= \frac{\beta_f}{f} m_{3/2}$ where β_f is the beta function for the corresponding superpotential Yukawa coupling. Anomaly-mediated contributions to scalar masses can also be derived and can be found in textbooks such as Ref. [12].

In cases where tree-level gravity-mediated soft terms are suppressed¹, then the AMSB contributions to soft SUSY breaking terms may dominate, leading to models with distinct phenomenological predictions. Famously, since gaugino masses are proportional to their gauge group beta functions, then one expects the $SU(3)_C$, $SU(2)_L$ and $U(1)_Y$ gaugino masses at the weak scale to occur in the ratios $M_3 : M_2 : M_1 \sim 8 : 1 : 3$ so that the wino is expected to be the lightest gaugino (as opposed to models with gaugino mass unification, where the bino is expected as the lightest gaugino). The advent of AMSB led to formulation of a minimal AMSB model (mAMSB)[14, 15] defined by parameters

$$m_0, m_{3/2}, \tan \beta, \text{sign}(\mu) \quad (\text{mAMSB}) \quad (2)$$

where a so-called *bulk* scalar mass contribution m_0 was postulated to avoid tachyonic sleptons. The magnitude of the superpotential μ parameter was tuned so as to generate the observed value of $m_Z = 91.2 \text{ GeV}$. The mAMSB model featured a wino-like lightest SUSY particle

¹Originally, sequestering the hidden sector from the visible sector via brane separation in extra dimensions was suggested[10]. There is still on-going debate regarding viable sequestration methods in SUSY models[13].

(LSP) and hence wino-like WIMP dark matter. The thermally underproduced wino-like WIMP abundance could be augmented to the measured DM abundance via moduli field decays in the early universe[16]. The mAMSB model provided a template for many investigations of how AMSB SUSY would manifest itself phenomenologically[17, 18, 19].

Nowadays, the mAMSB model seems highly implausible— perhaps even excluded— based on three counts:

1. The small $A_0 \sim 0$ parameter means little mixing of top-squarks so that the relatively large measured value of $m_h \simeq 125$ GeV can only be obtained by large, unnatural top-squark soft terms lying in the tens-to-hundreds of TeV regime[20, 21]. Such large stop masses lead to a naturalness problem[22].
2. A necessary condition for naturalness in SUSY models is that $\mu \sim m_{weak} \simeq m_{W,Z,h} \sim 100$ GeV. The large value of μ which is generated in mAMSB makes the model unnatural.
3. Limits on wino-like WIMP dark matter from indirect detection experiments effectively exclude wino-like LSPs[23, 24, 25] (although such constraints can be avoided by postulating mixed axion/wino dark matter (two DM particles)[26]).

In our discussion, it is essential to define what we mean by naturalness. Here, we adopt the (most conservative) electroweak naturalness measure Δ_{EW} . This measure depends on the computed value of m_Z from the scalar potential minimization conditions:

$$m_Z^2/2 = \frac{m_{H_d}^2 + \Sigma_d^d - (m_{H_u}^2 + \Sigma_u^u) \tan^2 \beta}{\tan^2 \beta - 1} - \mu^2 \simeq -m_{H_u}^2 - \mu^2 - \Sigma_u^u(\tilde{t}_{1,2}) \quad (3)$$

where the $\Sigma_{u,d}^{u,d}$ terms contain an assortment of loop corrections which are given in the Appendices of Ref's [27] and [28]. Δ_{EW} compares the largest term on the right-hand-side (RHS) of Eq. 3 to $m_Z^2/2$. If one (or more) term(s) on the RHS are far bigger than $m_Z^2/2$, then some other unrelated term will have to be opposite-sign but nearly same magnitude to maintain $m_Z = 91.2$ GeV. This is where the finetuning actually occurs in spectra generating computer codes. Older measures are problematic as explained in Ref. [29]. A value $\Delta_{EW} \lesssim 30$ corresponds to $\mu \lesssim 350$ GeV which coincides well with the Agrawal *et al.*[30] window of values (ABDS window) giving rise to anthropic selection of the magnitude of the weak scale on the string landscape[31].

A new phenomenological model dubbed *natural AMSB* (nAMSB) was proposed in Ref. [32] which incorporated two minor adjustments to mAMSB². First, there is no need for universality amongst the matter scalar masses, and in fact one of the hallmarks of SUGRA is that such terms are expected to be *non-universal*[33]. Thus, independent Higgs bulk terms were postulated such that $m_{H_u}^2 \neq m_{H_d}^2 \neq m_0(i)^2$ where $m_0(i)$ denotes the soft mass for each generation i of matter scalars. The independent high scale Higgs bulk soft terms can then be traded for the more convenient weak scale parameters μ and m_A . This allows for smaller values $\mu \sim 100 - 350$ GeV as required by weak scale naturalness[34]. Second, a bulk A_0 term is also allowed. Such a bulk A_0 term allows for large stop mixing which then allows for $m_h \sim 125$ GeV but with

²These minor adjustments were already suggested in the original RS paper[10].

top-squark masses in the few TeV range in accord with low $\Delta_{EW} \lesssim 30$. The parameter space of the retrofitted nAMSB model is thus given by

$$m_0(i), m_{3/2}, A_0, \tan\beta, \mu \text{ and } m_A \quad (\text{nAMSB}). \quad (4)$$

The nAMSB model thus allows for $m_h \sim 125$ GeV while $\Delta_{EW} \lesssim 30$, all while being in accord with LHC sparticle search constraints. Like the mAMSB model, the wino is still the lightest gaugino. Unlike mAMSB, the lightest higgsino is now the lightest electroweakino (EWino), and in fact the LSP. The higgsino-like LSP is also thermally underproduced. However, if naturalness is also required in the QCD sector, then the PQ solution[35, 36, 37] to the strong CP problem seems required and we expect mixed axion/higgsino-like WIMP dark matter[38] which avoids indirect dark matter detection constraints. Given the rearranged EWino mass hierarchy

$$m(\text{higgsino}) \ll m(\text{wino}) \ll m(\text{bino}) \ll m(\text{gluino}) \quad (5)$$

from nAMSB, the expected collider phenomenology also changes markedly from what was found in mAMSB. In particular, whereas the lightest neutral wino was expected to comprise DM in mAMSB, now in nAMSB both the neutral and charged winos are unstable and decay to vector or Higgs bosons plus the lighter higgsino states.

In Ref. [39], the expected collider phenomenology of nAMSB was investigated. LHC searches for gluino pair production in the context of simplified models[40, 41] are expected to apply to nAMSB. The Run 2 limit that $m_{\tilde{g}} \gtrsim 2.2$ TeV implies that $m_{3/2} \gtrsim 90$ TeV, thus providing a lower limit on expected $m_{3/2}$ values. Also, recent ATLAS searches for boosted hadronically-decaying EWinos[42] provided new limits on wino masses depending on the mass of the higgsinos where $m(\text{higgsinos}) \sim \mu$. For instance, for $\mu \sim 250$ GeV, then the range $m(\text{wino}) \sim 0.6 - 1$ TeV is excluded while for $\mu \sim 150$ GeV then $m(\text{wino}) \sim 0.5 - 1.02$ TeV is excluded. For lighter winos with $m \lesssim 0.5 - 0.6$ TeV, then the wino decay products are too soft and the searches become less efficient. The LHC limits on $m(\text{wino})$ correspond (in the case of $\mu \sim 250$ GeV) to limits on $m_{3/2} : 200 - 360$ TeV. Meanwhile, the naturalness limit $\Delta_{EW} \lesssim 30$ occurs for $m_{3/2} \lesssim 260$ TeV – within the LHC-excluded range from boosted hadronically-decaying EWino searches. Thus, at present there exists a *gap* in nAMSB parameter space $m_{3/2} : 90 - 200$ TeV where $m_h \sim 125$ GeV with $\Delta_{EW} \lesssim 30$ and which is allowed by present LHC search constraints.

The goal of the present paper is to ascertain if it is possible for LHC upgrades such as high luminosity LHC (pp collisions at $\sqrt{s} = 14$ TeV with 3000 fb^{-1} integrated luminosity) to *close the gap*, thus either discovering SUSY in its nAMSB incarnation or else ruling the model out. In pursuit of this goal, in Sec. 2 we first display the nAMSB parameter space in various parameter planes so as to delineate the remaining target model parameter space. Unlike natural SUSY models like the i -extra parameter non-universal Higgs model (NUHMi[27]) and natural generalized mirage mediation (nGMM[43]), it appears nAMSB is susceptible to complete exploration within its natural regions due to the presence of relatively light unstable winos which lead to several distinct collider search channels. In Sec. 3, we propose new nAMSB model lines for which we can explore LHC collider signals and SM backgrounds. In Sec. 4, we examine several LHC search channels which may help ATLAS/CMS close the gap. These include

- Soft opposite-sign dileptons from higgsino pair production,
- Same sign diboson $W^\pm W^\pm$ signature[44] arising from wino pair production,
- Hard isolated trileptons from wino pair production and
- top-squark pair production.

These channels may be used to fully explore the remaining gap in nAMSB model parameter space at HL-LHC. Our summary and conclusions follow in Sec. 5.

2 Overview of nAMSB parameter space

In many past works, the mAMSB model parameter space has been displayed in the m_0 vs. $m_{3/2}$ plane[15, 18, 19] for particular values of $\tan\beta$. The same can be performed for nAMSB except now the plane is sensitive to additional parameter possibilities. In Fig. 1, we present nAMSB parameter space in the $m_0(3)$ vs. $m_{3/2}$ plane where now we take the first/second generation bulk masses $m_0(1,2) \neq m_0(3)$, with $m_0(1,2) = 2m_0(3)$ and bulk trilinear $A_0 = 1.2m_0(3)$. The motivation here comes in part from expectations from SUGRA where non-universal bulk soft terms are expected, and the string landscape which would preferentially select large soft terms so long as they do not contribute too much to the determination of the weak scale (no large weak scale finetuning). We take each generation of matter scalars as degenerate since all elements of each generation fill out the 16-d spinor rep of $SO(10)$. The large first/second generation scalar masses which are expected actually can provide a landscape mixed decoupling/quasi-degeneracy solution to the SUSY flavor and CP problems[45].

Fig. 1 is portrayed for $\tan\beta = 10$ and $m_A = 2$ TeV, with *a*) $\mu = 150$ GeV and *b*) $\mu = 250$ GeV. We use Isajet 7.91 model 13 to compute spectra for the nAMSB model[46]. The left gray region is where sleptons become the LSP. Here, we assume *R*-parity conservation which is less ad-hoc than it used to be in that both *R*-parity and global $U(1)_{PQ}$ can arise from more fundamental discrete *R*-symmetries which provide simultaneously solutions both to the SUSY μ problem and also the axion quality problem[47, 48]. Thus, the left gray region is excluded. The lower gray region around $m_0(3) \sim 2000$ GeV is also excluded, this time because stop soft terms run tachyonic leading to charge and/or color breaking (CCB) minima in the scalar potential.

In Fig. 1, we also show contours of $m_h = 123$ and 127 GeV. Thus, the region between the $m_h : 123 - 127$ GeV contours is in accord with LHC m_h measurements (due to the large bulk $A = 0$ terms). We also show black contours of electroweak naturalness $\Delta_{EW} = 30$ and 50 . The regions below these contours are considered natural since all independent contributions to the weak scale are comparable to the weak scale (no finetuning needed for the LHP). The finetuning increases with $m_{3/2}$ since large $m_{3/2}$ yields a large value of $m_{\tilde{g}}$ and $m_{\tilde{t}_{1,2}}$ which in turn increases the $\Sigma_u^u(\tilde{t}_{1,2})$ contribution to the weak scale. Also, the region with too large $m_0(3)$ is excluded since the large stop sector soft terms lead to too large $\Sigma_u^u(\tilde{t}_{1,2})$ values.

The region of Fig. 1 below the orange contour labeled $m_{\tilde{g}} = 2.2$ TeV (for $m_{3/2} \lesssim 90 - 100$ TeV) is excluded by ATLAS/CMS limits on gluino pair production searches[49, 50]. The region between the two green contours labeled $m_{\tilde{\chi}_2^+} = 500, 600$ and 1000 GeV is excluded by the ATLAS search for EWinos which decay to W or Z which in turn decay hadronically[42]. This

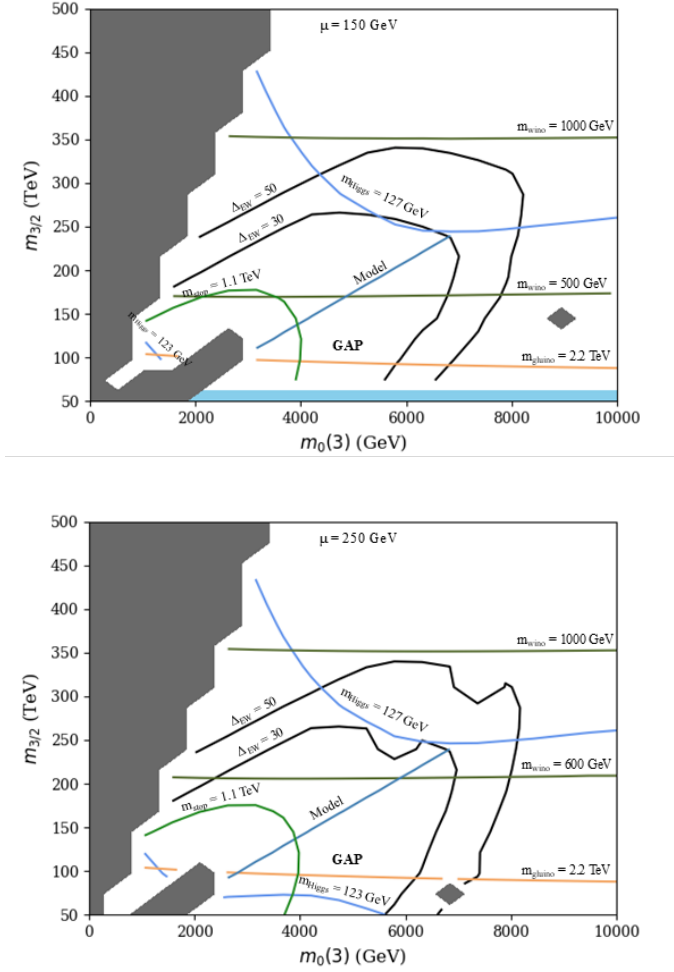


Figure 1: Plot of $m_0(3)$ vs. $m_{3/2}$ parameter space in the nAMSB model for $m_0(1, 2) = 2m_0(3)$, $A_0 = 1.2m_0(3)$ and $\tan \beta = 10$, with $m_A = 2$ TeV and a) $\mu = 150$ GeV and b) $\mu = 250$ GeV.

region includes the $\Delta_{EW} = 30$ and 50 contours and so, along with these contours, defines an upper limit to nAMSB parameter space (p-space). The remaining lower-left gap region is still allowed by naturalness, by the measured value of m_h , by direct/indirect mixed axion/higgsino-like WIMP dark matter searches[25] and by LHC sparticle search limits. This remaining gap provides a target for future LHC upgrade searches for the incarnation of natural SUSY via the nAMSB model.

In Fig. 2 we display the nAMSB parameter space in the A_0 vs. $m_{3/2}$ plane for fixed $m_0(3) = 5$ TeV and $m_0(1, 2) = 10$ TeV, with $\tan \beta = 10$ and $m_A = 2$ TeV with a) $\mu = 150$ GeV and b) $\mu = 250$ GeV (as before). Here, we find a right-side gray region where large values of A_0 cause $m_{U_3}^2$ to run tachyonic. The bulk of this p-space plane is unnatural with $\Delta_{EW} \gtrsim 50$ except for the region to the right of the naturalness contours. Also, we see that $m_h \sim 125$ GeV mainly on the right-hand-side unless $m_{3/2}$ is very large, in which case the spectra are unnatural. Here

it is plain to see the advantage that bulk trilinear terms provide: for $A_0 \sim 0$, then the model is unnatural and yields m_h too light unless $m_{3/2} \gtrsim 300$ TeV. We also show in the plot the orange contours of $m_{\tilde{g}} = 2.2$ TeV (below is excluded) and $m_{\tilde{\chi}_2^+} = 500, 600$ and 1000 GeV (between which is excluded). The remaining non-excluded target p-space lies on the extreme right where $A_0 \sim 5 - 7$ TeV.

3 An nAMSB model line

Our goal is to explore the LHC-allowed nAMSB parameter space with $\Delta_{EW} \lesssim 30$ to see if it is completely testable at HL-LHC. To this end, we construct a nAMSB model line that cuts through the bulk of allowed p-space but which varies with $m_{3/2}$ from the lower limit formed by LHC gluino pair searches to the upper limit which is formed by naturalness combined with LHC boosted hadronically-decaying EWino pair searches. Our constructed model line is shown in Fig. 1 as the blue diagonal line labeled *Model*. It is parametrized by

$$m_{3/2} = 35m_0(3) \quad (\text{nAMSB model line}) \quad (6)$$

with $m_0(1, 2) = 2m_0(3)$, $A_0 = 1.2m_0(3)$ and $\tan \beta = 10$ with $m_A = 2$ TeV and $\mu = 150$ GeV and 250 GeV.

In Fig. 3, we plot the value of m_h along the model line with $\mu = 250$ GeV, which extends from $m_{3/2} = 90$ TeV (left-most vertical red-dashed line) to $m_{3/2} \sim 210$ TeV (where LHC gaugino limits set in, denoted by the dashed red line at $m_{3/2} \sim 210$ TeV). From the plot, we see that m_h lies between 123-127 GeV, and so is consistent with the measured value of m_h up to a theory error of ± 2 GeV.

In Fig. 4, we plot the value of Δ_{EW} along the $\mu = 250$ GeV model line. In this case, we find that Δ_{EW} is typically between values of 15-30 along the line until it climbs beyond 30 (the red-dashed line) for $m_{3/2} \gtrsim 240$ TeV.

In Fig. 5, we plot various sparticle masses along the nAMSB model line. At the very bottom, the red and purple (nearly overlapping) curves denote the higgsino-like neutralinos $\tilde{\chi}_{1,2}^0$ and their masses are fixed to be very nearly $\sim \mu = 250$ GeV. The next-higher brown curve denotes the neutral wino $m_{\tilde{\chi}_3^0}^0 \sim M_2$ and these masses range between 275-600 GeV in the allowed region. Such light winos provide an inviting target for LHC searches since even higher values are already excluded by the LHC boosted EWino search results. The green curve shows the lighter top-squark mass $m_{\tilde{t}_1}$ which extends over the range $m_{\tilde{t}_1} : 0.6 - 2$ TeV. (The lower part of this range is already excluded by LHC top-squark searches within simplified models[49, 50].) The bino mass $m_{\tilde{\chi}_4^0}$ lies just above $m_{\tilde{t}_1}$ for this model line. Meanwhile, the gluino mass varies from $m_{\tilde{g}} : 2.2 - 4.5$ TeV while first/second generation sfermions lie in the 5-15 TeV range. For our HL-LHC search strategy, we will focus on the relatively light higgsinos and winos along this model line.

4 nAMSB discovery channels for HL-LHC

We next examine the reach of HL-LHC ($\sqrt{s} = 14$ TeV with 3000 fb^{-1}) for wino pair production in the nAMSB model. To proceed, we generate a SUSY Les Houches Accord (SLHA)

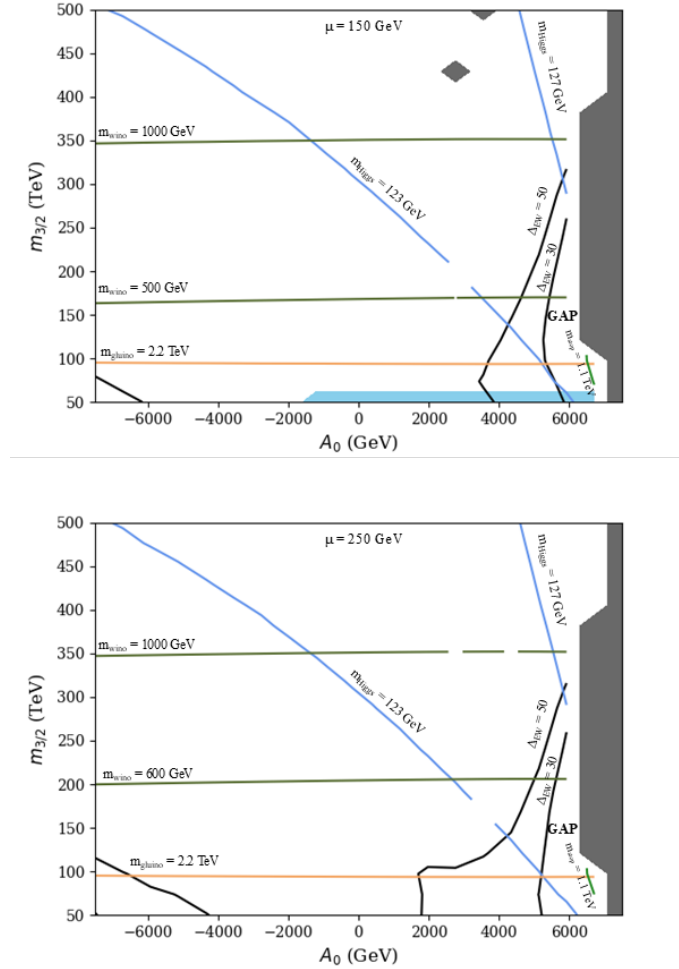


Figure 2: Plot of A_0 vs. $m_{3/2}$ parameter space in the nAMSB model for $m_0(3) = 5$ TeV with $m_0(1,2) = 2m_0(3)$ and $\tan\beta = 10$, with $m_A = 2$ TeV and a) $\mu = 150$ GeV and b) $\mu = 250$ GeV.

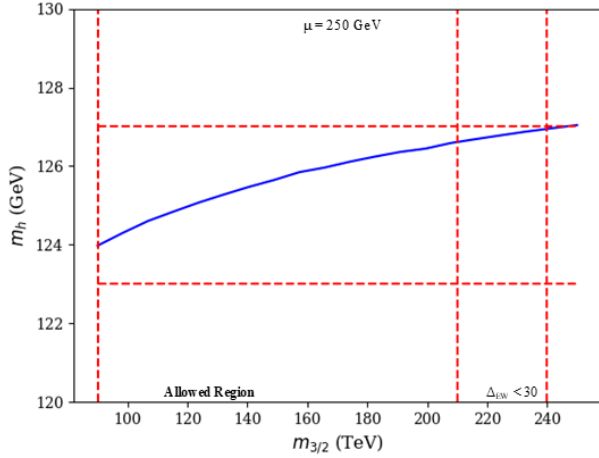


Figure 3: Plot of m_h vs. $m_{3/2}$ along the nAMSB model-line for $m_{3/2} = 35m_0(3)$ with $m_0(1, 2) = 2m_0(3)$, $A_0 = 1.2m_0(3)$ and $\tan \beta = 10$, with $\mu = 250$ GeV and $m_A = 2$ TeV.

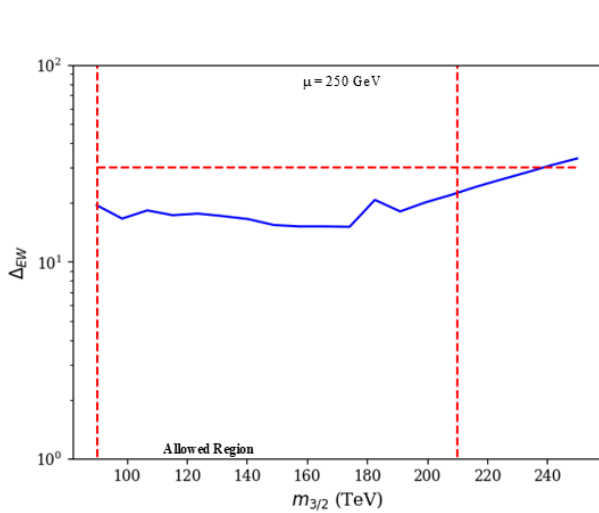


Figure 4: Plot of Δ_{EW} vs. $m_{3/2}$ along the nAMSB model-line for $m_{3/2} = 35m_0(3)$, $m_0(1, 2) = 2m_0(3)$, $A_0 = 1.2m_0(3)$ and $\tan \beta = 10$, with $\mu = 250$ GeV and $m_A = 2$ TeV.

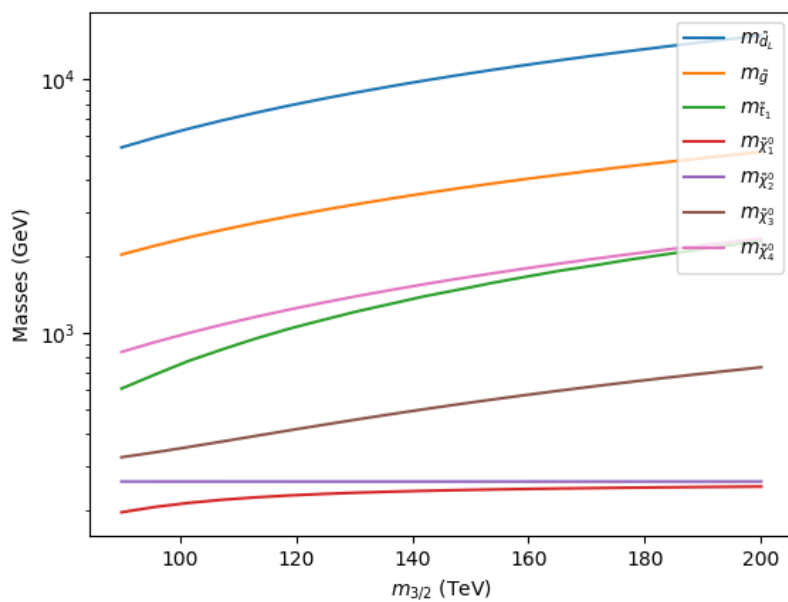


Figure 5: Plot of various sparticle masses vs. $m_{3/2}$ along the nAMSB model-line for $m_{3/2} = 35m_0(3)$ with $m_0(1, 2) = 2m_0(3)$, $A_0 = 1.2m_0(3)$ and $\tan\beta = 10$, with $\mu = 250$ GeV and $m_A = 2$ TeV.

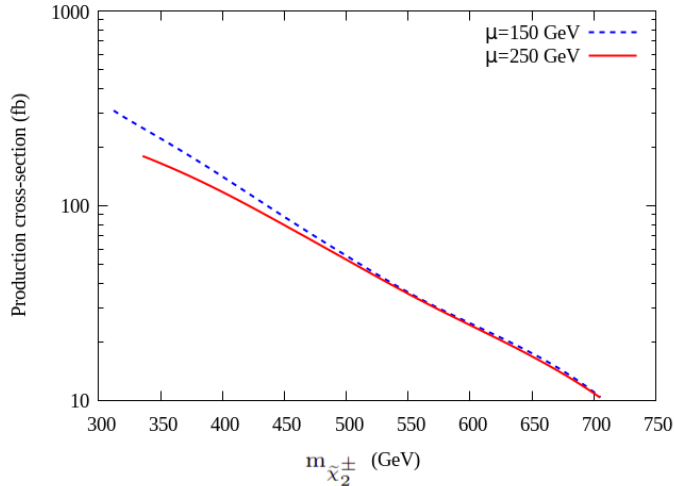


Figure 6: The production cross section from wino pair production $\tilde{\chi}_2^\pm \tilde{\chi}_3^0$ along the nAMSB model line with $\mu = 150$ and 250 GeV.

file[51] for each of our nAMSB SUSY model line points using Isajet 7.91[46] and feed this into Madgraph[52]/Pythia8[53] which is used for both signal and background (BG) processes. The $pp \rightarrow \tilde{\chi}_2^\pm \tilde{\chi}_3^0 X$ cross section is normalized to the Prospino NLO[54]. For the $2 \rightarrow 3$ BG processes, we also use Madgraph[52] coupled to Pythia. We adopt the toy detector simulation Delphes[55] using the default ATLAS card.

In Delphes, we identify the following entities.

- Jets are reconstructed using the anti- k_T algorithm with $p_T(j) > 20$ GeV within a cone of $\Delta R = 0.4$. Such clusters are labelled as jets when $p_T(j) > 40$ GeV with pseudorapidity $|\eta(j)| < 3.0$.
- Leptons with $p_T > 10$ GeV are reconstructed in a cone of $\Delta R = 0.2$. The maximum hadronic energy allowed in the cone is 10% of the leptonic p_T . Thus, leptons are identified when $p_T(\ell) > 10$ GeV and $|\eta(\ell)| < 2.5$.

4.1 Same-sign dileptons from wino pair production

Here we examine wino pair production $pp \rightarrow \tilde{\chi}_2^\pm \tilde{\chi}_3^0 X$ along our nAMSB model line at LHC14 where the relevant decay modes are $\tilde{\chi}_2^\pm \rightarrow \tilde{\chi}_{1,2}^0 W^\pm$ and $\tilde{\chi}_3^0 \rightarrow \tilde{\chi}_1^\pm W^\mp$. In this configuration, we expect a final state containing same-sign dibosons $W^\pm W^\pm + \cancel{E}_T$ about 50% of the time leading to a (relatively) jet-free same-sign dilepton + \cancel{E}_T signature for which SM backgrounds are typically quite low. The production cross-section for this channel at $\sqrt{s} = 14$ TeV LHC for two values of $\mu = 150, 250$ GeV are shown in Fig. 6. This signal channel- proposed in Ref. [44] and expanded upon in Ref. [56]– is endemic to SUSY models with light higgsinos although so far there are no dedicated experimental analyses. Here, we will adopt the signal cuts of Ref. [56]: The original cuts from Ref. [44] are labelled as cut set **C1** which require:

SM Bkg	Cross-section (after cuts) (ab)
$t\bar{t}$	0.0
$t\bar{t}t\bar{t}$	0.0125
$t\bar{t}W$	0.52
$t\bar{t}Z$	0.88
$WWjj$	2.21
WWW	2.21
WWZ	1.358
WZZ	1.426
ZZ	0.0
WZ	0.0
Total SM background	8.62

Table 1: The SM background cross-sections after cut **C2** for the same-sign dilepton + \cancel{E}_T signal at $\sqrt{s} = 14$ TeV.

- the presence of exactly two isolated same-sign leptons with $p_T(\ell_1) > 20$ GeV and $p_T(\ell_2) > 10$ GeV, where ℓ_1 (ℓ_2) is the higher (lower) p_T lepton,
- veto events with identified b -jets,
- $\cancel{E}_T > 200$ GeV and
- $\min(m_T(\ell_1, \cancel{E}_T), m_T(\ell_2, \cancel{E}_T)) > 175$ GeV.

After inspecting distributions for signal/background events, Ref. [56] augmented these with **C2** cuts:

- $n(jets) \leq 1$ and
- $\cancel{E}_T > 250$ GeV.

The backgrounds coming from $t\bar{t}$, WZ , $t\bar{t}W$, $t\bar{t}Z$, $t\bar{t}t\bar{t}$, WWW , $WWjj$, WWZ , WZZ and ZZ were computed and tabulated in Table II of Ref. [56]. The total background after cuts **C1** and **C2** (with all BG total cross sections scaled to their NLO results) was ~ 8.62 ab with the largest coming from WWW and $WWjj$ production at 2.21 ab as seen in Table 1.

The signal cross section after cuts **C2** is shown vs. $m_{\tilde{\chi}_2^\pm}$ along the nAMSB model line, for *a*) $\mu = 150$ and *b*) 250 GeV in Fig. 7. In Fig. 7a), we denote the total SM background by the solid red horizontal line at 8.6 ab while the HL-LHC $3000 \text{ fb}^{-1} 5\sigma$ line is horizontal red-dotted as is the 95%CL line. The left-most vertical line denotes the parameter space limit from LHC gluino pair searches where $m_{\tilde{g}} > 2.2$ TeV is required. The red-dotted vertical line at $m_{\tilde{\chi}_2^\pm} = 500, 600$ GeV denotes the upper limit on p-space from the ATLAS boosted hadronic jet search from wino pair production[42]. Beyond the right-most vertical red-dotted line is where the naturalness measure Δ_{EW} exceeds 30. From frame *a*), we see that for $\mu = 150$ GeV almost the entire presently-allowed p-space gap should be accessible to HL-LHC via the SSdB signal channel, well above the 5σ discovery limit (the exception being a tiny slice with low $m_{3/2}$ where decay products are rather soft and don't exceed our rather hard cuts; this small slice may be filled by updated gluino pair search results).

In Fig. 7b), we plot the SSdB signal rates for the same model line parameters except that $\mu = 250$ GeV. In the $\mu = 250$ GeV case, we see that the bulk of presently-allowed p-space can

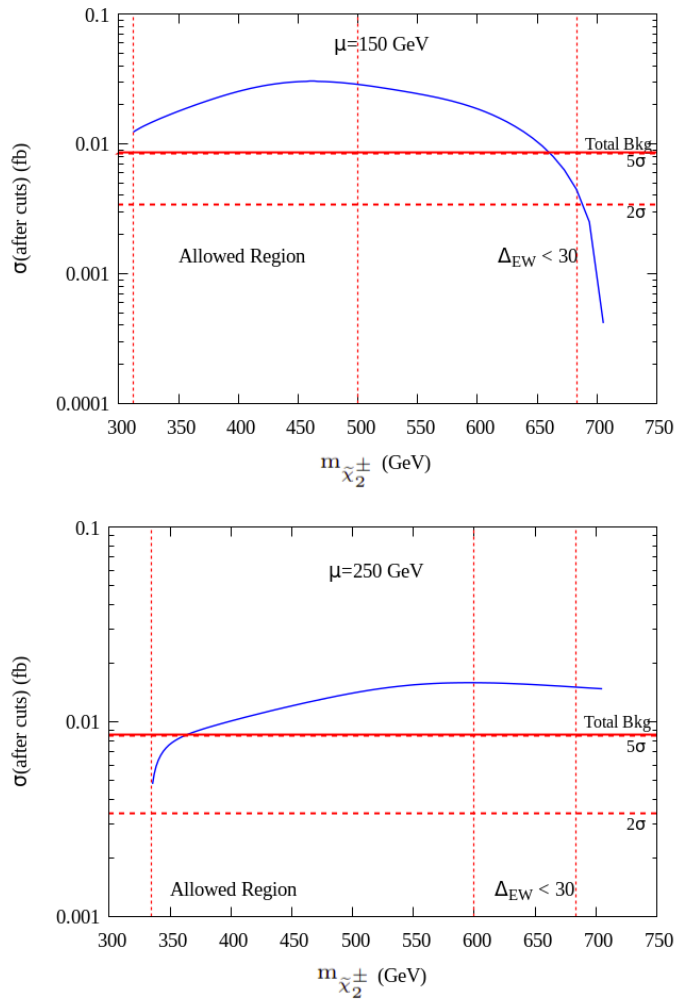


Figure 7: Cross section after cuts for the SSdB signature from wino pair production along the nAMSB model line for *a*) $\mu = 150$ GeV and *b*) $\mu = 250$ GeV. We also show the remaining total background rate.

be seen by HL-LHC at the 5σ level, except for the region with $m_{\tilde{\chi}_2^\pm} \lesssim 360$ GeV. For this lower range of wino mass values, the wino decays into real W s are still open, but the wino decay products are much softer, and a softer \cancel{E}_T cut may be necessary to pick out the lower mass wino pair events. In any case, the signal is only slightly below our projected 5σ level, and well above the 95%CL exclusion level.

4.2 Hard isolated trileptons from wino pair production

In this Subsection, we focus on wino pair production $pp \rightarrow \tilde{\chi}_2^\pm \tilde{\chi}_3^0$ followed by decays $\tilde{\chi}_2^\pm \rightarrow W^\pm \tilde{\chi}_{1,2}^0$ and $\tilde{\chi}_3^0 \rightarrow Z^0 \tilde{\chi}_{1,2}^0$. When both W and Z decay leptonically, then we expect the clean trilepton + \cancel{E}_T final state topology[57, 58].

We evaluate the signal and SM background using Madgraph/Pythia/Delphes as before. After examining signal and background distributions, we implement the following cuts

- The final state contains three identified isolated leptons with $p_T(\ell_1) > 20$ GeV, $p_T(\ell_2) > 15$ GeV and $p_T(\ell_3) > 10$ GeV, where ℓ_1 is the highest p_T lepton, and so forth.
- b -jet veto: $n_{b-jet} = 0$ and γ veto: $n_\gamma = 0$.
- $\cancel{E}_T > 100$ GeV.
- Effective mass $m_{eff} > 200$ GeV (where m_{eff} is the scalar sum of the p_T s of the three leptons plus the \cancel{E}_T).
- Transverse mass $m_T(\ell_i, \cancel{E}_T) > 120$ GeV for each isolated lepton $i = 1 - 3$.
- Jet veto: $n_j = 0$.

The various SM cross sections (normalized to their NLO values, and where available, up to NNLO+NNLL) after these cuts are listed in Table 4.2. The dominant backgrounds are summarized as below:

- $t\bar{t}$ - NNLO + NNLL [59]
- WZ, ZZ , - NLO [60]
- $t\bar{t}Z, t\bar{t}W$ - NLO (QCD + EW)[61]
- WWZ, WWW, ZZZ - NLO [62]
- tZj - NLO QCD+EW [63]
- tW - NNLO [64]

In Fig. 8a), we show a plot of the cross section after cuts along the nAMSB3 model line for $\mu = 150$ as a function of $m_{\tilde{\chi}_2^\pm}$, along with the total remaining SM background. We also show the 5σ and 95%CL reach of LHC14 for 3000 fb^{-1} of integrated luminosity. In this case, the wino pair production clean 3ℓ signal exceeds the 5σ level for $m_{\tilde{\chi}_2^\pm} \sim 300 - 620$ GeV, which

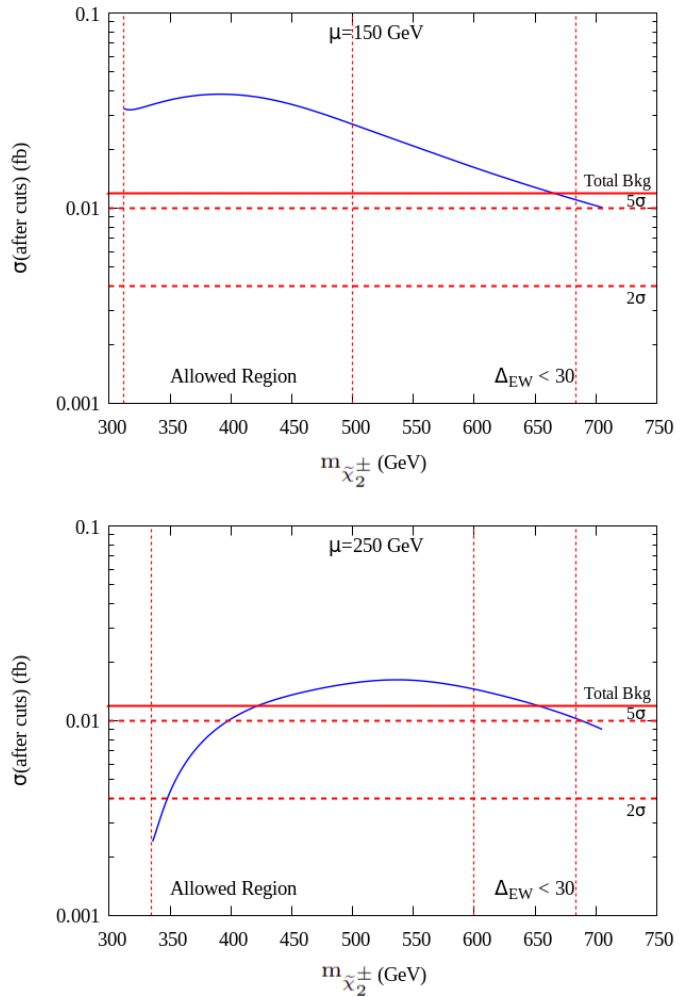


Figure 8: Cross section after cuts for the hard 3ℓ signature from wino pair production along the nAMSB model line with *a*) $\mu = 150$ GeV and *b*) $\mu = 250$ GeV. We also show the remaining total background rate. The central vertical dotted line corresponds to the LHC-allowed upper limit on p-space.

SM background	Cross-section after cuts (ab)
$t\bar{t}$	2.92
WZ	0.712
ZZ	0.45
ttZ	2.25
ttW	0.32
WWZ	5.12
WWW	0.035
ZZZ	0.0047
tZj	0.158
tW	0
Total Background	11.97

Table 2: Cross section after cuts in ab for the dominant SM backgrounds to the hard 3ℓ signal at LHC14.

is the entire allowed gap. A signal in this channel would provide strong confirmation of any signal already present in the SSdB channel.

In Fig. 8b), we show the hard 3ℓ signal along the nAMSB model line but with $\mu = 250$ GeV. In this case, the signal exceeds the 5σ level for the more limited range of $m_{\tilde{\chi}_2^\pm} \sim 450 - 600$ GeV. Thus, the lower portion of the gap is more difficult to access due to the softer wino decay products, since the wino decay to real W bosons is just barely open. Nonetheless, the signal exceeds the 95%CL range except for the very lowest values of $m_{\tilde{\chi}_2^\pm} \lesssim 350$ GeV,

4.3 Soft OS dileptons from higgsino pair production

Next we turn to nAMSB signals from higgsino pair production. The most lucrative reaction in this case comes from[65]

$$pp \rightarrow \tilde{\chi}_1^0 \tilde{\chi}_2^0 \quad \text{with} \quad \tilde{\chi}_2^0 \rightarrow \tilde{\chi}_1^0 \ell \bar{\ell}. \quad (7)$$

The visible decay products are very soft since the mass gap $m_{\tilde{\chi}_2^0} - m_{\tilde{\chi}_1^0}$ tends to be in the 5-50 GeV range, and most of the $\tilde{\chi}_2^0$ decay energy release goes into making the $\tilde{\chi}_1^0$ rest mass. The final state lepton energy can be boosted to higher values, and events can be triggered upon, by requiring a hard ISR jet emission[66, 67]. This is then the soft OS dilepton plus jet plus MET signature (OSDLJMET). Five selection cuts plus a ditau reconstruction cut requiring $m_{\tau\tau}^2 < 0$ to reject backgrounds such as Zj production (followed by $Z \rightarrow \tau\bar{\tau}$) were required in Ref. [67]. In Ref. [68], more efficient angular cuts were developed which reduce the ditau backgrounds to tiny levels. The original cut set **C1** augmented by new angular cuts to reject $Zj \rightarrow \tau\bar{\tau}j$ plus further cuts to reject $t\bar{t}$ and WW backgrounds were labelled set **C3** in Ref. [68, 69]. After cut-set **C3**, signal and SM BG were plotted against opposite-sign dilepton invariant mass $m(\ell\bar{\ell})$ where signal should accrue for $m(\ell\bar{\ell}) < m_{\tilde{\chi}_2^0} - m_{\tilde{\chi}_1^0}$ whilst for higher invariant masses data should be in accord with SM expectations.

In the present work, we evaluate signal along the nAMSB model lines for $\mu = 150$ GeV and 250 GeV using cuts **C3** along with the dilepton invariant mass edge cut and compare to SM backgrounds as evaluated in Ref's [68, 69]. Our results are shown in Fig. 9a) and b) for $\mu = 150$ and 250 GeV, respectively. From Fig. 9a) for $\mu = 150$ GeV, we see the blue signal curve lies well above the 5σ BG level for LHC14 with 3 ab^{-1} over the whole gap region. However, in

frame *b*) for $\mu = 250$ GeV, the higgsino pair production signal is below the 5σ level for the entire allowed range of $m_{3/2}$ although it is above the 95%CL level for $m_{3/2} \sim 125 - 210$ TeV.

In Fig. 10 we show in frame *a*) the cross section for the OSDJMET signal after cuts **C3** of Ref. [68] and with $m(\ell\bar{\ell}) < m_{\tilde{\chi}_2^0} - m_{\tilde{\chi}_1^0}$. As μ increases, while M_2 is fixed in this plot, then the light higgsinos become increasingly mixed and the mass gap $m_{\tilde{\chi}_2^0} - m_{\tilde{\chi}_1^0}$ also increases so that the BG increases as well. But for 3 ab^{-1} of integrated luminosity, the number of signal events remain above 30 even for the maximal value of $\mu \sim 350$ GeV. In frame *b*), we show the $n\sigma$ level for the OSDJMET signal after cuts for LHC14 with 3 ab^{-1} of integrated luminosity. Here we show that the OSDJMET signal is above the 5σ discovery level out to $\mu \sim 225$ GeV and it lies above the 95%CL exclusion level for $\mu \lesssim 280$ GeV. For higher μ values, a signal in the OSDJMET channel would be difficult to ascertain.

4.4 Top-squark pair production

For light top-squarks, along the nAMSB model lines we have the $\tilde{t}_1 \rightarrow t\tilde{\chi}_1^0$ and $b\tilde{\chi}_1^+$ decay modes open, as is usual in natural models with gaugino mass unification, such as NUHM3. The difference between nAMSB and NUHM3 is that for nAMSB, the decay modes $\tilde{t}_1 \rightarrow b\tilde{\chi}_2^+$ and $\tilde{t}_1 \rightarrow t\tilde{\chi}_3^0$ may also be open at the 5-10% level, leading to some differences from expectations for NUHM3. The reach of HL-LHC for light top squarks $pp \rightarrow \tilde{t}_1\tilde{t}_1^*X$ was computed in Ref. [70] and the 5σ reach was found to extend to $m_{\tilde{t}_1} \lesssim 1.7$ TeV and the 95%CL reach to $m_{\tilde{t}_1} \lesssim 2$ TeV. We do not expect the results for the reach along the nAMSB model line to differ much from the NUHM3 model projections.

5 Summary and conclusions

Anomaly-mediated gaugino masses are expected in a class of models where some sort of sequestering of tree-level gaugino masses occurs, such as in models with charged SUSY breaking (no hidden sector singlets[11]). In contrast, in such models scalar masses are expected to occur at tree-level with $m_\phi \sim m_{3/2}$ since any remnant hidden sector symmetries do not suppress these in the Kähler potential. While the original mAMSB model now seems excluded by naturalness bounds combined with requiring $m_h \sim 125$ GeV and bounds on wino-like WIMP dark matter, an alternative generalized AMSB model which is characterized by non-universal bulk scalar masses and bulk A -terms is fully allowed. The nAMSB model still has winos as the lightest gauginos, but now higgsinos are the lightest EWinos, in accord with naturalness. The presence of rather light winos in this class of models has already led to strong bounds on the higher range of wino masses from LHC gaugino searches with hadronically-decaying boosted W s and Z s, the excluded range of which encompasses the $\Delta_{EW} \lesssim 30$ naturalness limit. This leaves an allowed parameter space gap between lower limits on $m_{3/2}$ from LHC gluino pair production searches to upper limits from the boosted hadronically decaying W, Z searches.

We investigated here whether or not this intermediate gap of allowed p-space can be fully probed at HL-LHC. Our answer is that yes it can, mainly based on the light winos expected in nAMSB which give rise to a distinctive SSdB signal (leading to hadronically quiet same-sign dileptons plus missing transverse energy) with very tiny SM backgrounds. Usually this

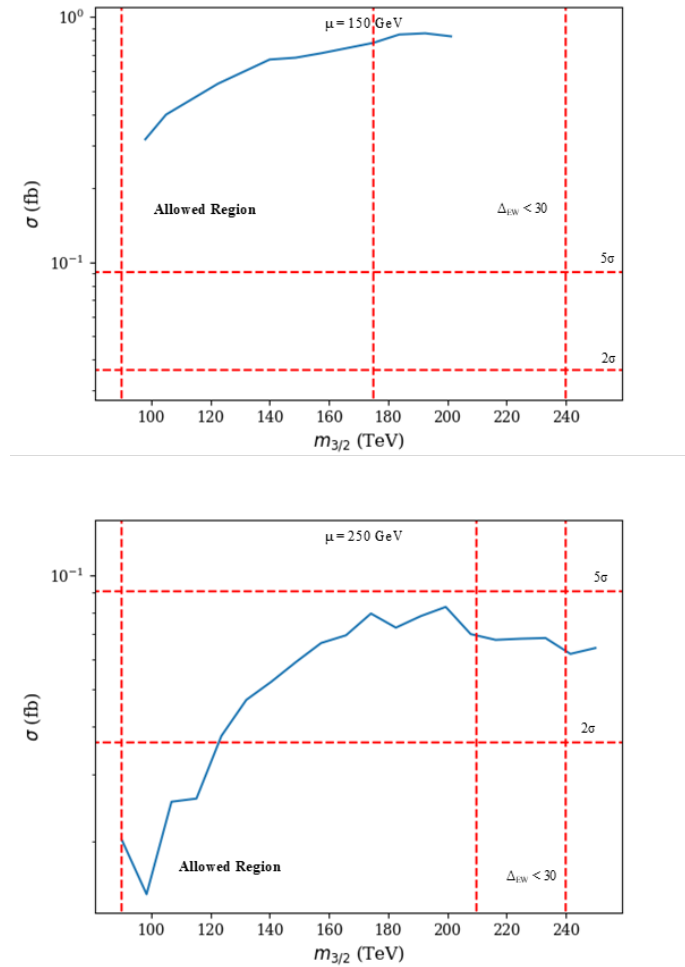


Figure 9: Cross section after cuts for the soft opposite-sign dilepton plus jet plus \cancel{E}_T events from higgsino pair production along the nAMSB model line with *a*) $\mu = 150$ GeV and *b*) $\mu = 250$ GeV. We also show the 5σ and 95%CL lines for HL-LHC with 3 ab^{-1} of integrated luminosity.

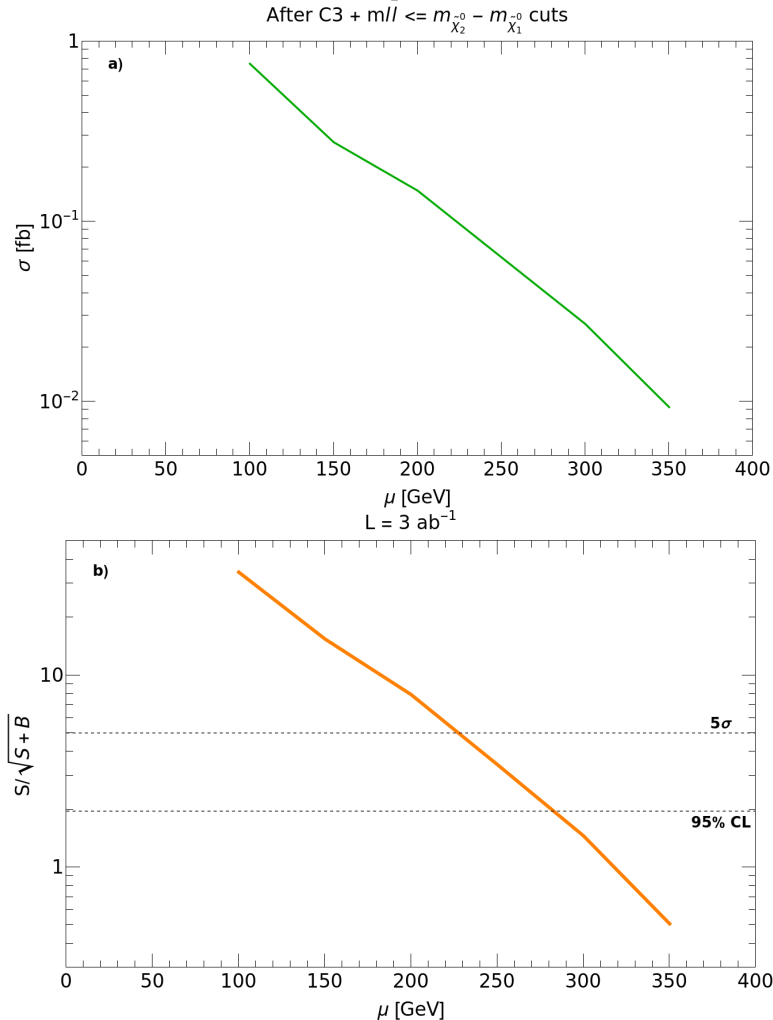


Figure 10: Cross section after cuts for the soft opposite-sign dilepton plus jet plus \cancel{E}_T events from higgsino pair production along the nAMSB model line vs. μ but with $m_{3/2} = 150$ TeV, $m_0(3) = m_{3/2}/35$, $m_0(1, 2) = 2m_0(3)$, $A_0 = 1.2m_0(3)$, $m_A = 2$ TeV and $\tan \beta = 10$. In *a*), we show remaining signal cross section after cuts **C3** of Ref. [68] but with $m(\ell\bar{\ell}) < m_{\tilde{\chi}_2^0} - m_{\tilde{\chi}_1^0}$, and in frame *b*), we show the n - σ value after cuts at LHC14 with 3 ab^{-1} of integrated luminosity.

signal should exceed the 5σ discovery level unless higgsinos are on the heavy side, whence the visible final state energy is degraded. Specialized cuts for this regime may boost it back to the 5σ discovery range. Along with the SSdB signal, over much of p-space a hard 3ℓ signal arising from wino pair production should also be visible. Also, for not-too-heavy higgsinos, then the soft dilepton plus jet signal from higgsino pair production should be visible. Top-squarks with mass $m_{\tilde{t}_1} \lesssim 1.8$ TeV may also be visible to HL-LHC. Taken together, it seems HL-LHC can either discover or at least rule out nAMSB. This is different from other natural models such as NUHM3 with unified gaugino masses or generalized mirage mediation with compressed gaugino masses where it seems sparticles may lie beyond HL-LHC reach while still fulfilling the naturalness requirement of $\Delta_{EW} \lesssim 30$ [71].

Acknowledgments

HB gratefully acknowledges support from the Avenir foundation. VB gratefully acknowledges support from the William F. Vilas Estate.

References

- [1] H. P. Nilles, Supersymmetry, Supergravity and Particle Physics, *Phys. Rept.* 110 (1984) 1–162. [doi:10.1016/0370-1573\(84\)90008-5](https://doi.org/10.1016/0370-1573(84)90008-5).
- [2] D. J. H. Chung, L. L. Everett, G. L. Kane, S. F. King, J. D. Lykken, L.-T. Wang, The Soft supersymmetry breaking Lagrangian: Theory and applications, *Phys. Rept.* 407 (2005) 1–203. [arXiv:hep-ph/0312378](https://arxiv.org/abs/hep-ph/0312378), [doi:10.1016/j.physrep.2004.08.032](https://doi.org/10.1016/j.physrep.2004.08.032).
- [3] E. Cremmer, S. Ferrara, L. Girardello, A. Van Proeyen, Yang-Mills Theories with Local Supersymmetry: Lagrangian, Transformation Laws and SuperHiggs Effect, *Nucl. Phys. B* 212 (1983) 413. [doi:10.1016/0550-3213\(83\)90679-X](https://doi.org/10.1016/0550-3213(83)90679-X).
- [4] G. 't Hooft, Naturalness, chiral symmetry, and spontaneous chiral symmetry breaking, *NATO Sci. Ser. B* 59 (1980) 135–157. [doi:10.1007/978-1-4684-7571-5_9](https://doi.org/10.1007/978-1-4684-7571-5_9).
- [5] E. Witten, Dynamical Breaking of Supersymmetry, *Nucl. Phys. B* 188 (1981) 513. [doi:10.1016/0550-3213\(81\)90006-7](https://doi.org/10.1016/0550-3213(81)90006-7).
- [6] H. Baer, V. Barger, D. Martinez, S. Salam, Practical naturalness and its implications for weak scale supersymmetry, *Phys. Rev. D* 108 (3) (2023) 035050. [arXiv:2305.16125](https://arxiv.org/abs/2305.16125), [doi:10.1103/PhysRevD.108.035050](https://doi.org/10.1103/PhysRevD.108.035050).
- [7] M. Dine, J. D. Mason, Supersymmetry and Its Dynamical Breaking, *Rept. Prog. Phys.* 74 (2011) 056201. [arXiv:1012.2836](https://arxiv.org/abs/1012.2836), [doi:10.1088/0034-4885/74/5/056201](https://doi.org/10.1088/0034-4885/74/5/056201).
- [8] H. P. Nilles, Gaugino Condensation and Supersymmetry Breakdown, *Int. J. Mod. Phys. A* 5 (1990) 4199–4224. [doi:10.1142/S0217751X90001744](https://doi.org/10.1142/S0217751X90001744).

- [9] I. Affleck, M. Dine, N. Seiberg, Dynamical Supersymmetry Breaking in Four-Dimensions and Its Phenomenological Implications, *Nucl. Phys. B* 256 (1985) 557–599. [doi:10.1016/0550-3213\(85\)90408-0](https://doi.org/10.1016/0550-3213(85)90408-0).
- [10] L. Randall, R. Sundrum, Out of this world supersymmetry breaking, *Nucl. Phys. B* 557 (1999) 79–118. [arXiv:hep-th/9810155](https://arxiv.org/abs/hep-th/9810155), [doi:10.1016/S0550-3213\(99\)00359-4](https://doi.org/10.1016/S0550-3213(99)00359-4).
- [11] G. F. Giudice, M. A. Luty, H. Murayama, R. Rattazzi, Gaugino mass without singlets, *JHEP* 12 (1998) 027. [arXiv:hep-ph/9810442](https://arxiv.org/abs/hep-ph/9810442), [doi:10.1088/1126-6708/1998/12/027](https://doi.org/10.1088/1126-6708/1998/12/027).
- [12] H. Baer, X. Tata, Weak scale supersymmetry: From superfields to scattering events, Cambridge University Press, 2006.
- [13] M. Dine, N. Seiberg, Comments on quantum effects in supergravity theories, *JHEP* 03 (2007) 040. [arXiv:hep-th/0701023](https://arxiv.org/abs/hep-th/0701023), [doi:10.1088/1126-6708/2007/03/040](https://doi.org/10.1088/1126-6708/2007/03/040).
- [14] T. Gherghetta, G. F. Giudice, J. D. Wells, Phenomenological consequences of supersymmetry with anomaly induced masses, *Nucl. Phys. B* 559 (1999) 27–47. [arXiv:hep-ph/9904378](https://arxiv.org/abs/hep-ph/9904378), [doi:10.1016/S0550-3213\(99\)00429-0](https://doi.org/10.1016/S0550-3213(99)00429-0).
- [15] J. L. Feng, T. Moroi, Supernatural supersymmetry: Phenomenological implications of anomaly mediated supersymmetry breaking, *Phys. Rev. D* 61 (2000) 095004. [arXiv:hep-ph/9907319](https://arxiv.org/abs/hep-ph/9907319), [doi:10.1103/PhysRevD.61.095004](https://doi.org/10.1103/PhysRevD.61.095004).
- [16] T. Moroi, L. Randall, Wino cold dark matter from anomaly mediated SUSY breaking, *Nucl. Phys. B* 570 (2000) 455–472. [arXiv:hep-ph/9906527](https://arxiv.org/abs/hep-ph/9906527), [doi:10.1016/S0550-3213\(99\)00748-8](https://doi.org/10.1016/S0550-3213(99)00748-8).
- [17] F. E. Paige, J. D. Wells, Anomaly mediated SUSY breaking at the LHC, in: 1st Les Houches Workshop on Physics at TeV Colliders, 1999. [arXiv:hep-ph/0001249](https://arxiv.org/abs/hep-ph/0001249).
- [18] H. Baer, J. K. Mizukoshi, X. Tata, Reach of the CERN LHC for the minimal anomaly mediated SUSY breaking model, *Phys. Lett. B* 488 (2000) 367–372. [arXiv:hep-ph/0007073](https://arxiv.org/abs/hep-ph/0007073), [doi:10.1016/S0370-2693\(00\)00925-4](https://doi.org/10.1016/S0370-2693(00)00925-4).
- [19] A. J. Barr, C. G. Lester, M. A. Parker, B. C. Allanach, P. Richardson, Discovering anomaly mediated supersymmetry at the LHC, *JHEP* 03 (2003) 045. [arXiv:hep-ph/0208214](https://arxiv.org/abs/hep-ph/0208214), [doi:10.1088/1126-6708/2003/03/045](https://doi.org/10.1088/1126-6708/2003/03/045).
- [20] A. Arbey, M. Battaglia, A. Djouadi, F. Mahmoudi, J. Quevillon, Implications of a 125 GeV Higgs for supersymmetric models, *Phys. Lett. B* 708 (2012) 162–169. [arXiv:1112.3028](https://arxiv.org/abs/1112.3028), [doi:10.1016/j.physletb.2012.01.053](https://doi.org/10.1016/j.physletb.2012.01.053).
- [21] H. Baer, V. Barger, P. Huang, D. Mickelson, A. Mustafayev, X. Tata, Post-LHC7 fine-tuning in the minimal supergravity/CMSSM model with a 125 GeV Higgs boson, *Phys. Rev. D* 87 (3) (2013) 035017. [arXiv:1210.3019](https://arxiv.org/abs/1210.3019), [doi:10.1103/PhysRevD.87.035017](https://doi.org/10.1103/PhysRevD.87.035017).

[22] H. Baer, V. Barger, D. Mickelson, M. Padeffke-Kirkland, SUSY models under siege: LHC constraints and electroweak fine-tuning, *Phys. Rev. D* 89 (11) (2014) 115019. [arXiv:1404.2277](#), doi:10.1103/PhysRevD.89.115019.

[23] T. Cohen, M. Lisanti, A. Pierce, T. R. Slatyer, Wino Dark Matter Under Siege, *JCAP* 10 (2013) 061. [arXiv:1307.4082](#), doi:10.1088/1475-7516/2013/10/061.

[24] J. Fan, M. Reece, In Wino Veritas? Indirect Searches Shed Light on Neutralino Dark Matter, *JHEP* 10 (2013) 124. [arXiv:1307.4400](#), doi:10.1007/JHEP10(2013)124.

[25] H. Baer, V. Barger, H. Serce, SUSY under siege from direct and indirect WIMP detection experiments, *Phys. Rev. D* 94 (11) (2016) 115019. [arXiv:1609.06735](#), doi:10.1103/PhysRevD.94.115019.

[26] K. J. Bae, H. Baer, A. Lessa, H. Serce, Mixed axion-wino dark matter, *Front. in Phys.* 3 (2015) 49. [arXiv:1502.07198](#), doi:10.3389/fphy.2015.00049.

[27] H. Baer, V. Barger, P. Huang, D. Mickelson, A. Mustafayev, X. Tata, Radiative natural supersymmetry: Reconciling electroweak fine-tuning and the Higgs boson mass, *Phys. Rev. D* 87 (11) (2013) 115028. [arXiv:1212.2655](#), doi:10.1103/PhysRevD.87.115028.

[28] H. Baer, V. Barger, D. Martinez, Comparison of SUSY spectra generators for natural SUSY and string landscape predictions, *Eur. Phys. J. C* 82 (2) (2022) 172. [arXiv:2111.03096](#), doi:10.1140/epjc/s10052-022-10141-2.

[29] H. Baer, V. Barger, D. Mickelson, How conventional measures overestimate electroweak fine-tuning in supersymmetric theory, *Phys. Rev. D* 88 (9) (2013) 095013. [arXiv:1309.2984](#), doi:10.1103/PhysRevD.88.095013.

[30] V. Agrawal, S. M. Barr, J. F. Donoghue, D. Seckel, Viable range of the mass scale of the standard model, *Phys. Rev. D* 57 (1998) 5480–5492. [arXiv:hep-ph/9707380](#), doi:10.1103/PhysRevD.57.5480.

[31] H. Baer, V. Barger, H. Serce, K. Sinha, Higgs and superparticle mass predictions from the landscape, *JHEP* 03 (2018) 002. [arXiv:1712.01399](#), doi:10.1007/JHEP03(2018)002.

[32] H. Baer, V. Barger, D. Sengupta, Anomaly mediated SUSY breaking model retrofitted for naturalness, *Phys. Rev. D* 98 (1) (2018) 015039. [arXiv:1801.09730](#), doi:10.1103/PhysRevD.98.015039.

[33] S. K. Soni, H. A. Weldon, Analysis of the Supersymmetry Breaking Induced by N=1 Supergravity Theories, *Phys. Lett. B* 126 (1983) 215–219. doi:10.1016/0370-2693(83)90593-2.

[34] H. Baer, V. Barger, P. Huang, A. Mustafayev, X. Tata, Radiative natural SUSY with a 125 GeV Higgs boson, *Phys. Rev. Lett.* 109 (2012) 161802. [arXiv:1207.3343](#), doi:10.1103/PhysRevLett.109.161802.

[35] R. D. Peccei, H. R. Quinn, CP Conservation in the Presence of Instantons, *Phys. Rev. Lett.* 38 (1977) 1440–1443. [doi:10.1103/PhysRevLett.38.1440](https://doi.org/10.1103/PhysRevLett.38.1440).

[36] S. Weinberg, A New Light Boson?, *Phys. Rev. Lett.* 40 (1978) 223–226. [doi:10.1103/PhysRevLett.40.223](https://doi.org/10.1103/PhysRevLett.40.223).

[37] F. Wilczek, Problem of Strong P and T Invariance in the Presence of Instantons, *Phys. Rev. Lett.* 40 (1978) 279–282. [doi:10.1103/PhysRevLett.40.279](https://doi.org/10.1103/PhysRevLett.40.279).

[38] K. J. Bae, H. Baer, E. J. Chun, Mainly axion cold dark matter from natural supersymmetry, *Phys. Rev. D* 89 (3) (2014) 031701. [arXiv:1309.0519](https://arxiv.org/abs/1309.0519), [doi:10.1103/PhysRevD.89.031701](https://doi.org/10.1103/PhysRevD.89.031701).

[39] H. Baer, V. Barger, J. Bolich, J. Dutta, D. Sengupta, Natural anomaly mediation from the landscape with implications for LHC SUSY searches, *Phys. Rev. D* 109 (3) (2024) 035011. [arXiv:2311.18120](https://arxiv.org/abs/2311.18120), [doi:10.1103/PhysRevD.109.035011](https://doi.org/10.1103/PhysRevD.109.035011).

[40] T. C. Collaboration, et al., Search for supersymmetry in proton-proton collisions at 13 TeV in final states with jets and missing transverse momentum, *JHEP* 10 (2019) 244. [arXiv:1908.04722](https://arxiv.org/abs/1908.04722), [doi:10.1007/JHEP10\(2019\)244](https://doi.org/10.1007/JHEP10(2019)244).

[41] Search for squarks and gluinos in final states with jets and missing transverse momentum using 139 fb^{-1} of $\sqrt{s} = 13 \text{ TeV}$ pp collision data with the ATLAS detector.

[42] G. Aad, et al., Search for charginos and neutralinos in final states with two boosted hadronically decaying bosons and missing transverse momentum in pp collisions at $\sqrt{s} = 13 \text{ TeV}$ with the ATLAS detector, *Phys. Rev. D* 104 (11) (2021) 112010. [arXiv:2108.07586](https://arxiv.org/abs/2108.07586), [doi:10.1103/PhysRevD.104.112010](https://doi.org/10.1103/PhysRevD.104.112010).

[43] H. Baer, V. Barger, H. Serce, X. Tata, Natural generalized mirage mediation, *Phys. Rev. D* 94 (11) (2016) 115017. [arXiv:1610.06205](https://arxiv.org/abs/1610.06205), [doi:10.1103/PhysRevD.94.115017](https://doi.org/10.1103/PhysRevD.94.115017).

[44] H. Baer, V. Barger, P. Huang, D. Mickelson, A. Mustafayev, W. Sreethawong, X. Tata, Same sign diboson signature from supersymmetry models with light higgsinos at the LHC, *Phys. Rev. Lett.* 110 (15) (2013) 151801. [arXiv:1302.5816](https://arxiv.org/abs/1302.5816), [doi:10.1103/PhysRevLett.110.151801](https://doi.org/10.1103/PhysRevLett.110.151801).

[45] H. Baer, V. Barger, D. Sengupta, Landscape solution to the SUSY flavor and CP problems, *Phys. Rev. Res.* 1 (3) (2019) 033179. [arXiv:1910.00090](https://arxiv.org/abs/1910.00090), [doi:10.1103/PhysRevResearch.1.033179](https://doi.org/10.1103/PhysRevResearch.1.033179).

[46] F. E. Paige, S. D. Protopopescu, H. Baer, X. Tata, ISAJET 7.69: A Monte Carlo event generator for pp , $\text{anti-}p$ p , and e^+e^- reactions [arXiv:hep-ph/0312045](https://arxiv.org/abs/hep-ph/0312045).

[47] H. Baer, V. Barger, D. Sengupta, Gravity safe, electroweak natural axionic solution to strong CP and SUSY μ problems, *Phys. Lett. B* 790 (2019) 58–63. [arXiv:1810.03713](https://arxiv.org/abs/1810.03713), [doi:10.1016/j.physletb.2019.01.007](https://doi.org/10.1016/j.physletb.2019.01.007).

[48] P. N. Bhattachiprolu, S. P. Martin, High-quality axions in solutions to the μ problem, *Phys. Rev. D* 104 (5) (2021) 055014. [arXiv:2106.14964](https://arxiv.org/abs/2106.14964), doi:10.1103/PhysRevD.104.055014.

[49] A. Canepa, Searches for Supersymmetry at the Large Hadron Collider, *Rev. Phys.* 4 (2019) 100033. doi:10.1016/j.revph.2019.100033.

[50] G. Aad, et al., The quest to discover supersymmetry at the ATLAS experiment [arXiv:2403.02455](https://arxiv.org/abs/2403.02455).

[51] P. Z. Skands, et al., SUSY Les Houches accord: Interfacing SUSY spectrum calculators, decay packages, and event generators, *JHEP* 07 (2004) 036. [arXiv:hep-ph/0311123](https://arxiv.org/abs/hep-ph/0311123), doi:10.1088/1126-6708/2004/07/036.

[52] J. Alwall, M. Herquet, F. Maltoni, O. Mattelaer, T. Stelzer, MadGraph 5 : Going Beyond, *JHEP* 06 (2011) 128. [arXiv:1106.0522](https://arxiv.org/abs/1106.0522), doi:10.1007/JHEP06(2011)128.

[53] T. Sjostrand, S. Mrenna, P. Z. Skands, PYTHIA 6.4 Physics and Manual, *JHEP* 05 (2006) 026. [arXiv:hep-ph/0603175](https://arxiv.org/abs/hep-ph/0603175), doi:10.1088/1126-6708/2006/05/026.

[54] W. Beenakker, R. Hopker, M. Spira, PROSPINO: A Program for the production of supersymmetric particles in next-to-leading order QCD [arXiv:hep-ph/9611232](https://arxiv.org/abs/hep-ph/9611232).

[55] J. de Favereau, C. Delaere, P. Demin, A. Giannanco, V. Lemaître, A. Mertens, M. Selvaggi, DELPHES 3, A modular framework for fast simulation of a generic collider experiment, *JHEP* 02 (2014) 057. [arXiv:1307.6346](https://arxiv.org/abs/1307.6346), doi:10.1007/JHEP02(2014)057.

[56] H. Baer, V. Barger, J. S. Gainer, M. Savoy, D. Sengupta, X. Tata, Aspects of the same-sign diboson signature from wino pair production with light higgsinos at the high luminosity LHC, *Phys. Rev. D* 97 (3) (2018) 035012. [arXiv:1710.09103](https://arxiv.org/abs/1710.09103), doi:10.1103/PhysRevD.97.035012.

[57] H. Baer, X. Tata, Multi - Lepton Signals From W^\pm and Z^0 Decays to Gauginos at $\bar{p}p$ Colliders, *Phys. Lett. B* 155 (1985) 278–283. doi:10.1016/0370-2693(85)90654-9.

[58] H. Baer, C.-h. Chen, F. Paige, X. Tata, Trileptons from chargino - neutralino production at the CERN Large Hadron Collider, *Phys. Rev. D* 50 (1994) 4508–4516. [arXiv:hep-ph/9404212](https://arxiv.org/abs/hep-ph/9404212), doi:10.1103/PhysRevD.50.4508.

[59] M. Czakon, A. Mitov, Top++: A Program for the Calculation of the Top-Pair Cross-Section at Hadron Colliders, *Comput. Phys. Commun.* 185 (2014) 2930. [arXiv:1112.5675](https://arxiv.org/abs/1112.5675), doi:10.1016/j.cpc.2014.06.021.

[60] J. M. Campbell, R. K. Ellis, C. Williams, Vector Boson Pair Production at the LHC, *JHEP* 07 (2011) 018. [arXiv:1105.0020](https://arxiv.org/abs/1105.0020), doi:10.1007/JHEP07(2011)018.

[61] D. de Florian, et al., Handbook of LHC Higgs Cross Sections: 4. Deciphering the Nature of the Higgs Sector 2/2017. [arXiv:1610.07922](https://arxiv.org/abs/1610.07922), doi:10.23731/CYRM-2017-002.

[62] J. Alwall, R. Frederix, S. Frixione, V. Hirschi, F. Maltoni, O. Mattelaer, H. S. Shao, T. Stelzer, P. Torrielli, M. Zaro, The automated computation of tree-level and next-to-leading order differential cross sections, and their matching to parton shower simulations, JHEP 07 (2014) 079. [arXiv:1405.0301](https://arxiv.org/abs/1405.0301), doi:10.1007/JHEP07(2014)079.

[63] D. Pagani, I. Tsinikos, E. Vryonidou, NLO QCD+EW predictions for tHj and tZj production at the LHC, JHEP 08 (2020) 082. [arXiv:2006.10086](https://arxiv.org/abs/2006.10086), doi:10.1007/JHEP08(2020)082.

[64] N. Kidonakis, Theoretical results for electroweak-boson and single-top production, PoS DIS2015 (2015) 170. [arXiv:1506.04072](https://arxiv.org/abs/1506.04072), doi:10.22323/1.247.0170.

[65] H. Baer, V. Barger, P. Huang, Hidden SUSY at the LHC: the light higgsino-world scenario and the role of a lepton collider, JHEP 11 (2011) 031. [arXiv:1107.5581](https://arxiv.org/abs/1107.5581), doi:10.1007/JHEP11(2011)031.

[66] Z. Han, G. D. Kribs, A. Martin, A. Menon, Hunting quasidegenerate Higgsinos, Phys. Rev. D 89 (7) (2014) 075007. [arXiv:1401.1235](https://arxiv.org/abs/1401.1235), doi:10.1103/PhysRevD.89.075007.

[67] H. Baer, A. Mustafayev, X. Tata, Monojet plus soft dilepton signal from light higgsino pair production at LHC14, Phys. Rev. D 90 (11) (2014) 115007. [arXiv:1409.7058](https://arxiv.org/abs/1409.7058), doi:10.1103/PhysRevD.90.115007.

[68] H. Baer, V. Barger, D. Sengupta, X. Tata, New angular and other cuts to improve the Higgsino signal at the LHC, Phys. Rev. D 105 (9) (2022) 095017. [arXiv:2109.14030](https://arxiv.org/abs/2109.14030), doi:10.1103/PhysRevD.105.095017.

[69] H. Baer, V. Barger, D. Sengupta, X. Tata, Angular cuts to reduce the $\tau\bar{\tau}j$ background to the higgsino signal at the LHC, in: Snowmass 2021, 2022. [arXiv:2203.03700](https://arxiv.org/abs/2203.03700).

[70] H. Baer, V. Barger, J. Dutta, D. Sengupta, K. Zhang, Top squarks from the landscape at high luminosity LHC, Phys. Rev. D 108 (7) (2023) 075027. [arXiv:2307.08067](https://arxiv.org/abs/2307.08067), doi:10.1103/PhysRevD.108.075027.

[71] H. Baer, V. Barger, S. Salam, D. Sengupta, K. Sinha, Status of weak scale supersymmetry after LHC Run 2 and ton-scale noble liquid WIMP searches, Eur. Phys. J. ST 229 (21) (2020) 3085–3141. [arXiv:2002.03013](https://arxiv.org/abs/2002.03013), doi:10.1140/epjst/e2020-000020-x.